The EMBO Journal Vol. 21 No. 22 pp. 6225–6235, 2002

'Super p53' mice exhibit enhanced DNA damage response, are tumor resistant and age normally

Isabel García-Cao, Marta García-Cao, Juan Martín-Caballero[1], Luis M.Criado, Peter Klatt, Juana M.Flores[2], Jean-Claude Weill[3], María A.Blasco and Manuel Serrano[4]

Spanish National Center of Biotechnology, Department of Immunology and Oncology, Campus de Cantoblanco, Madrid E-28049, [1]Spanish National Center of Oncology, Melchor Fernández Almagro 3, Madrid E-28029, [2]Complutense University of Madrid, Veterinary School, Madrid E-28040, Spain and [3]INSERM U373-Faculté de Medecine Necker-Enfants Malades, 156 rue de Vaugirard, 75730 Paris Cedex 15, France

[4]Corresponding author
e-mail: mserrano@cnb.uam.es

The tumor suppressor p53 is critical in preventing cancer due to its ability to trigger proliferation arrest and cell death upon the occurrence of a variety of stresses, most notably, DNA damage and oncogenic stress. Here, we report the generation and characterization of mice carrying supernumerary copies of the p53 gene in the form of large genomic transgenes. Prior to this, we demonstrate that the p53 transgenic allele (p53-tg), when present in a p53-null genetic background, behaves as a functional replica of the endogenous gene. 'Super p53' mice, carrying p53-tg alleles in addition to the two endogenous alleles, exhibit an enhanced response to DNA damage. Importantly, 'super p53' mice are significantly protected from cancer when compared with normal mice. Finally, in contrast to previously reported mice with constitutively active p53, 'super p53' mice do not show any indication of premature aging, probably reflecting the fact that p53 is under normal regulatory control. Together, our results prove that cancer resistance can be enhanced by a simple genetic modification and in the absence of undesirable effects.

Keywords: aging/animal models/DNA damage/p53/tumor suppression

Introduction

Tumor suppressor genes (TSGs) are key components of the cancer protection mechanisms (Hanahan and Weinberg, 2000). Their most significant characteristic is the fact that they are inactivated frequently in tumors through stochastic, genetic and/or epigenetic, mutational processes. Indeed, for a given TSG, two mutational events are generally observed in tumors, each inactivating a different allele. In agreement with this, individuals carrying a germline-mutated allele of a TSG have significantly increased cancer susceptibility. Following a parallel reasoning, it is anticipated that increasing the gene dosage of a TSG, regardless of other possible effects, should translate into a lower probability of inactivating that particular TSG and, therefore, into a lower incidence of cancer.

While the approach of eliminating TSGs from mice is used extensively for cancer research, the opposite approach of increasing their gene dosage has been hampered in the past by the difficulties in reproducing exactly the transcriptional regulation of an endogenous gene. 'Classical' transgenes generally are formed by a short promoter region followed by the cDNA of interest and, thus, lack distant regulatory or structural elements (Giraldo and Montoliu, 2001). As a consequence, 'classical' transgenes almost invariably exhibit aberrant regulation. For example, 'classical' p53 transgenes resulted in dramatic overexpression of p53 restricted to particular cell types, thus producing atrophy of the target organ (Nakamura *et al*., 1995; Godley *et al*., 1996; Allemand *et al*., 1999). During the past years, obtaining large genomic segments has been facilitated by a new generation of vectors, such as bacterial artificial chromosomes (BACs), that can accommodate long DNA inserts (>100 kb). Using this approach, it is possible to obtain 'genomic' transgenic animals in which, regardless of the integration site, the transgenes reproduce the normal expression and regulation of the endogenous gene counterpart (Giraldo and Montoliu, 2001).

The TSG p53 is a highly attractive and informative candidate for the generation of a mouse model with an increased gene dosage. The function of p53 is to prevent cellular proliferation in the face of cellular damage (Vogelstein *et al*., 2000). For this, p53 is expressed ubiquitously in all cell types as an inactive, latent, transcription factor that becomes active only when the cells are subjected to a variety of cellular insults. Two main groups of signals activate p53, namely DNA damage (signaled through the ATM and Chk kinases) and oncogenic stress (signaled through the p53-stabilizing protein ARF) (Sherr, 1998; Prives and Hall, 1999; Sharpless and DePinho, 1999; Woods and Vousden, 2001). The activation of p53 triggers a complex transcriptional program that, depending on the cellular type and context, leads to proliferation arrest or death by apoptosis. DNA damage and oncogenic stress are universally associated with cancer and, therefore, it is assumed that p53 activation occurs always at some point during tumor development. In agreement with its central role in tumor suppression, p53 is the most frequently mutated TSG in human cancers of different types (overall frequency of ~50%). Interestingly, those tumors that have not inactivated p53 directly have hampered its functionality by mutating components of the signaling pathways that activate p53, as is often the case for ARF (Prives and Hall, 1999; Sharpless and DePinho, 1999; Woods and Vousden, 2001).

The proliferation arrest induced by p53 can be permanent, as happens when telomeres are exhausted and chromosomal ends become uncapped (a type of arrest called 'replicative senescence'), or upon severe cellular damage (a process sometimes referred to as 'stress-induced cellular senescence') (Serrano and Blasco, 2001). The induction of cellular senescence in response to stress is designed to prevent the proliferation of damaged cells for the benefit of the organism. However, it is conceivable that an excess of p53 function could eventually translate into a premature onset of organismal aging. In this regard, the phenotype of mice containing a large deletion that eliminates an undetermined number of genes together with the 5′-half of the p53 gene has been reported recently (Tyner *et al*., 2002). Mice heterozygous for this deletion have a decreased incidence of spontaneous tumors, but age prematurely (Tyner *et al*., 2002). It has been proposed that these phenotypes could be due to a truncated p53 protein which, in turn, could result in constitutive activation of wild-type p53 (Tyner *et al*., 2002). Similarly, mice overexpressing large amounts of a partially active mutant p53 also present some signs of premature aging (Tyner *et al*., 2002). Together, these results support the idea that constitutively active p53 could have an effect on organismal aging.

Here, we describe the generation of mice with an increased gene dosage of p53, but, importantly, which retain normal regulation of p53. In this manner, we demonstrate that it is possible to provide a stronger response to DNA damage and to increase cancer resistance without accelerating the normal aging process. We anticipate that these mice will constitute a useful animal model to study p53, tumor suppression and cancer resistance.

Results

Strategy for the generation of 'super p53' mice

In order to keep the expression properties of p53 as intact as possible, we performed transgenesis using large DNA segments containing the p53 gene in its natural genomic context. Two genomic segments containing p53 were isolated from a mouse genomic library in BACs. Sequencing of the genomic terminal regions adjacent to the BAC vector and comparison with the ENSEMBL Mouse Genome Database was sufficient to determine the precise limits of the genomic segments. In the case of BAC p53-tg, the genomic segment is 130 kb long and the p53 transcriptional unit is located in a terminal position (Figure 1A). In BAC p53-tg^{b}, the genomic insert is 175 kb long and p53 is in a central position. Two lines of transgenic mice were obtained, one for each genomic segment, which were named p53-tg and p53-tg^{b}, respectively. Southern blotting with a probe to detect a terminal region of each transgene indicated correspondingly that the mouse line p53-tg contained a single copy of the transgene (Figure 1B), and that line p53-tg^{b} contained two copies (Figure 1C) that were genetically linked along generations, probably due to a tandem arrangement, as is usually the case. We have focused most of our efforts on the detailed characterization of p53-tg, which serves here as a model to study the consequences of increasing the gene dosage of p53 under conditions that retain its normal regulation. We also present confirmatory characterization for the second transgenic line, p53-tg^{b}. As shown below, the behavior of these two lines of p53 transgenic mice is in agreement with an extensive literature indicating that genes contained in large genomic transgenes reproducibly behave as the endogenous counterparts, independently of their integration site and in proportion to the number of transgenic copies (Giraldo and Montoliu, 2001).

Rescue of p53 deficiency in MEFs

To test the functionality of the p53-tg allele, we performed the appropriate crosses to place the transgene in a p53-null background ($p53^{-/-;tg/\cdot}$). The resulting mice were used to obtain mouse embryo fibroblasts (MEFs) that were used to perform a number of assays for p53 function. Due to the low levels of expression of p53 in MEFs, we first measured the basal expression of the p53 transcriptional target $p21^{Waf1/Cip1}$, which is known to be dependent on p53 (Macleod *et al*., 1995). This analysis indicated that $p53^{-/-;tg/\cdot}$ MEFs have rescued the normal basal levels of p21 (Figure 2A). We also evaluated the inducibility of p53 in response to DNA damage (Figure 2B). $p53^{-/-;tg/\cdot}$ MEFs clearly induced p53 upon treatment with the genotoxic agent adriamycin, and at levels quantitatively comparable with those of $p53^{+/-}$ MEFs (Figure 2B). Exposure of MEFs to DNA damage results in a proliferative arrest that is mostly dependent on the ATM/p53/p21 pathway and that is reflected by a lower rate of bromodeoxyuridine (BrdU) incorporation (Brugarolas *et al*., 1995; Deng *et al*., 1995; Wang *et al*., 1997; Xu *et al*., 1998). Evaluation of BrdU incorporation in γ-irradiated MEFs of different genotypes demonstrated that the G_1/S checkpoint activated by p53 is completely restored by the p53-tg allele (Figure 2C).

Continued cultivation of MEFs under standard *in vitro* conditions eventually triggers a stress-related response that results in a permanent cell cycle arrest mediated by the ARF/p53 pathway (Sherr and DePinho, 2000). This phenomenon is generally referred to as 'crisis' or 'senescence' (Sherr and DePinho, 2000; Serrano and Blasco, 2001), and is manifested by low colony formation efficiency and the inability to expand primary cultures serially beyond a certain point. In agreement with the role of p53 in senescence/crisis, $p53^{+/+}$ or $p53^{+/-}$ MEFs have a very low colony formation efficiency compared with $p53^{-/-}$ MEFs (Figure 2D). Importantly, $p53^{-/-;tg/\cdot}$ MEFs behaved like MEFs with functional p53 (Figure 2D). Serial passage of independent MEF cultures also indicated that the p53-tg allele is functional. In particular, six independent cultures of $p53^{-/-}$ or $p53^{+/-}$ MEFs, three of each genotype, did not show evidence of senescence/crisis, as expected (Harvey *et al*., 1993a; Tsukada *et al*., 1993; see an example in Figure 2E). It should be noted that heterozygous $p53^{+/-}$ MEFs are not strictly immortal, but the observation of a senescence/crisis phase is precluded by the high frequency of loss of the wild-type allele (Harvey *et al*., 1993a). Significantly, independent cultures of $p53^{+/-;tg/\cdot}$ MEFs (n = 3) behaved very similarly to wild-type MEFs (n = 3), all of them showing a clear senescence/crisis phase (see an example in Figure 2E). To prove further the functionality of the p53-tg allele during senescence/crisis, we examined whether loss of the transgene was associated frequently with immortalization. Indeed, Southern blot analysis indicated frequent loss of

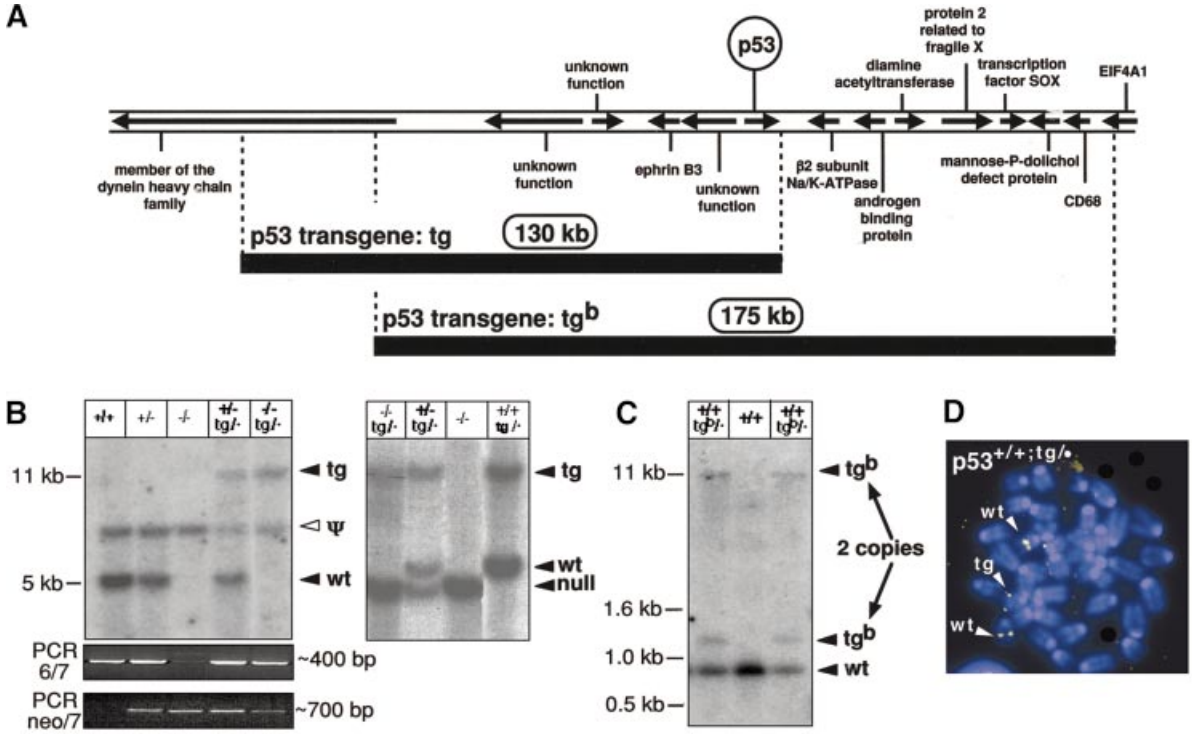

Fig. 1. Strategy to increase the gene dosage of p53. (**A**) Map of the genomic segments used to generate the 'super p53' mice. The map is based on the ENSEMBL Mouse Genome Database and shows the approximate position of the transcriptional units surrounding the p53 gene. The exact position of the limits of the two BACs used in this work was determined from their terminal sequences. The sizes of the two genomic inserts were determined experimentally by pulsed-field electrophoresis, and both are compatible with the predicted sizes from the ENSEMBL Mouse Genome Database. (**B**) Identification of the p53-tg allele by Southern blotting. *Sca*I-digested genomic DNA from mice of the indicated genotypes was hybridized with a probe that detects either exon 6 of p53 (absent in the p53 null allele; see Jacks *et al*., 1994; and Supplementary data) (left panel) or a region immediately downstream of exon 11 (after the p53 transcriptional unit; see Supplementary data) (right panel). These strategies allow the detection of fragments containing the junction between BAC-p53-tg and the surrounding DNA at the insertion site (see Supplementary data). Genotyping was confirmed further in combination with PCR data, according to the strategy described in Jacks *et al*. (1994) to amplify the region between exons 6 and 7 (present in the wild-type and tg alleles) and the region between the neo marker and exon 7 (present in the null allele) (bottom panels). The existence of a p53 pseudogene detected with exonic probes is well established (see for example Jacks *et al*., 1994), and the band resulting from it (marked as Ψ) is common to all DNA preparations independently of p53 genotype. Mice carrying the p53-tg allele exhibit a single additional band in both types of Southern blots (marked as tg), indicative of a single BAC-p53-tg copy. (**C**) Identification of the p53-tg^b allele by Southern blotting. *Eco*RI-digested genomic DNA from mice of the indicated genotypes was hybridized with a probe that detects a terminal fragment of BAC-p53-tg^b. This strategy allows the detection of fragments containing the junction between BAC-p53-tg^b and the surrounding DNA at the insertion site (see Supplementary data). Mice carrying the p53-tg^b allele exhibit two additional bands (marked as tg^b), indicative of two BAC-p53-tg^b copies. These two copies co-segregated along mouse generations, indicating that they are genetically linked. (**D**) Identification of the p53-tg allele by fluorescence *in situ* hybridization (FISH). Representative example of a metaphase derived from p53$^{+/+;tg/\cdot}$ MEFs and hybridized with the entire BAC-p53-tg. The endogenous alleles are known to be located at a central region in chromosome pair 11. Control metaphases from wild-type mice gave only two pairs of signals at a central position (data not shown). In the p53$^{+/+;tg/\cdot}$ metaphases, a third pair of signals appears located in the telomeric region of a non-identified chromosome.

p53-tg (four out of six cultures) in spontaneously p53$^{-/-;tg/\cdot}$ and p53$^{+/-;tg/\cdot}$ immortalized MEFs (Figure 2F).

We considered another assay for p53 functionality consisting of the protection from Ras-mediated neoplastic transformation. It is well established that, in MEFs, the ARF/p53 pathway is essential for the anti-oncogenic response elicited by activated Ras alleles (Serrano *et al*., 1997; Palmero *et al*., 1998). Consequently, p53$^{+/+}$ or p53$^{+/-}$ MEFs are refractory to the formation of neoplastic foci upon transfection of RasV12, whereas p53$^{-/-}$ MEFs readily form foci. Importantly, the p53-tg allele rendered MEFs lacking endogenous p53 significantly resistant to Ras-induced neoplastic transformation (Figure 2G).

Together, the above data indicate that, in the context of MEFs, the p53-tg allele rescues all the tested phenotypes, namely normal expression of p21, normal responses to DNA damage and stress, and resistance to oncogenic transformation by Ras.

Rescue of p53 deficiency in mice

The functionality of the p53-tg allele was next examined in the context of the organism. First, p53$^{-/-;tg/\cdot}$ mice survive for times well beyond their p53$^{-/-}$ littermates. In particular, p53$^{-/-;tg/\cdot}$ mice had an average lifespan of 9.5 months (n = 9), a value that is significantly longer than the average latency of our control colony of p53$^{-/-}$ mice (4.5 months, n = 11). Indeed, the earliest observed death of a p53$^{-/-;tg/\cdot}$ mouse happened at 7 months of age, a time when essentially all the p53$^{-/-}$ mice have succumbed to tumors (Harvey *et al*., 1993b; Jacks *et al*., 1994). Nonetheless, it is interesting to note that the average lifespan of p53$^{-/-;tg/\cdot}$ mice (9.5 months, n = 9) was shorter than that of p53$^{+/-}$ mice (14.0 months, n = 8). At first sight, this might suggest that the *in vivo* tumor suppression potency of the transgene is diminished compared with the endogenous allele. However, an important factor to consider is the frequency of loss of heterozygosity (LOH) of the

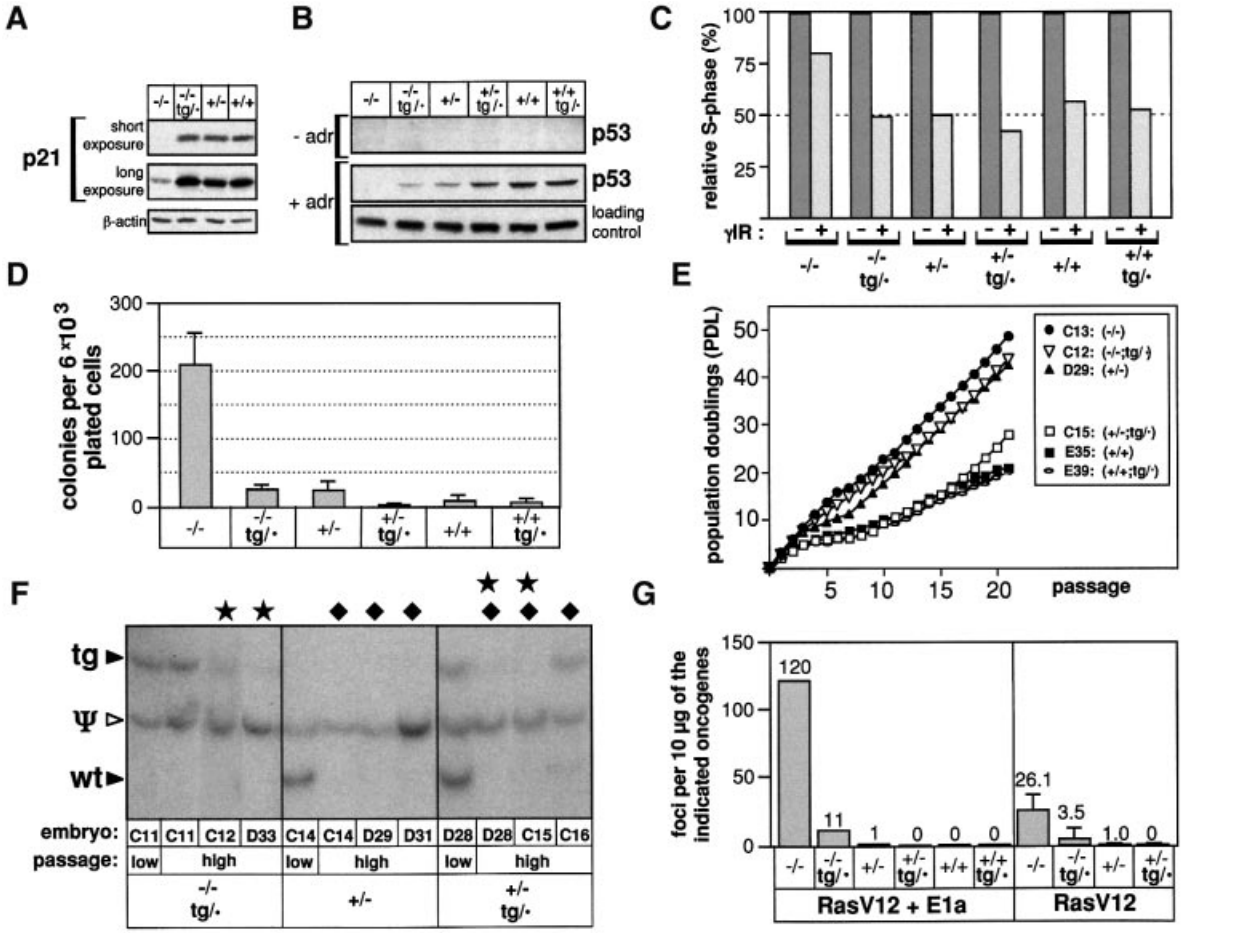

Fig. 2. Rescue of phenotypes associated with p53-null MEFs. (**A**) The p53-tg allele rescues basal p21 protein levels in $p53^{-/-;tg/\cdot}$ MEFs. Protein extracts of early-passage MEFs of the indicated genotypes were analyzed by immunoblot to determine the levels of p21. Two exposures of the same immunoblot are shown to reveal the levels of p21 in $p53^{-/-}$ MEFs. The same blot was re-probed with β-actin to evaluate protein loading. (**B**) $p53^{-/-;tg/\cdot}$ MEFs respond to DNA damage by stabilizing p53 to levels comparable with those of $p53^{+/-}$ cells. Early-passage MEFs of the indicated genotypes were left untreated (–adr) or treated with adriamycin (+adr) (see Supplementary data). Protein extracts were analyzed by immunoblot to determine the basal and inducible levels of p53. For simplicity, the β-actin loading control is only shown for the treated cells. (**C**) The p53-tg allele rescues cell cycle arrest in response to DNA damage. Asynchronously proliferating cultures of early-passage MEFs of the indicated genotypes were γ-irradiated (5.5 Gy) and the proportion of cells in S phase was measured 18 h later by BrdU incorporation and cell cytometry. The figure shows the relative change in the S-phase compartment with respect to non-irradiated cells. (**D**) The colony formation efficiency of primary $p53^{-/-;tg/\cdot}$ MEFs is comparable with that of $p53^{+/-}$ MEFs. Early passage MEFs of the indicated genotypes were plated at low density and the total number of colonies formed was scored after 2 weeks. For each genotype, three independently isolated MEF cultures were used, and the figure shows the average and SD of the three values. (**E**) $p53^{+/-;tg/\cdot}$ MEFs enter senescence/crisis upon serial cultivation in a manner similar to $p53^{+/+}$ MEFs. The figure shows the profile of accumulated population doublings (PDL) corresponding to individual cultures, each representative of a different genotype, as indicated. A total of three cultures were derived from each genotype, but only one is shown for simplicity. (**F**) Loss of the p53-tg allele in immortalized MEF cultures. Southern blotting of *Sca*I-digested genomic DNA from cultures of the indicated genotypes, at passage 0 (abbreviated as 'low') and passage 21 (abbreviated as 'high') (see E), and hybridized with p53 exon 6 (see Figure 1B). The intensity of the bands corresponding to the wild-type (wt) and transgenic (tg) alleles was compared with the band of the pseudogene (Ψ) (used as an internal reference). Complete or partial losses of the p53-tg (stars) or the p53-wt (diamonds) alleles are indicated. (**G**) $p53^{-/-;tg/\cdot}$ MEFs are similar to $p53^{+/-}$ MEFs in their resistance to neoplastic transformation *in vitro*. Early-passage MEFs of the indicated genotypes were transfected with a combination of RasV12 and adenoviral E1a, or simply with RasV12 (see Supplementary data). The total number of neoplastic foci was scored after 3 weeks. In the case of RasV12 plus E1a, the assay was performed with only one MEF culture for each genotype. In the case of RasV12 alone, the assay was performed in triplicate using three independently isolated MEF cultures for each genotype, and the figure shows the average and SD of the three values.

transgene compared with the endogenous allele. In murine cells, LOH occurs mainly by mitotic recombination between homologous chromosomes and, consequently, the frequency of LOH of a given genetic marker increases with the distance from the centromere (e.g. see Shao *et al*., 1999). In the particular case of the p53-tg allele, its position has been determined to be at a telomeric region (see Figure 1D), while the endogenous allele is located centrally in a chromosome arm. These differences in the distance to the centromere predict that LOH of the transgene should occur more frequently than LOH of the endogenous gene, and this may explain, at least in part, the comparatively shorter tumor latency of the $p53^{-/-;tg/\cdot}$ mice compared with $p53^{+/-}$ mice.

We have explored in detail the DNA damage response of $p53^{-/-;tg/\cdot}$ mice. For this, animals were subjected to whole-body γ-irradiation, and the p21 mRNA levels were analyzed in various tissues as a surrogate indicator of p53 functionality (Macleod *et al*., 1995). This analysis turned out to be extremely sensitive to the variations in p53 gene

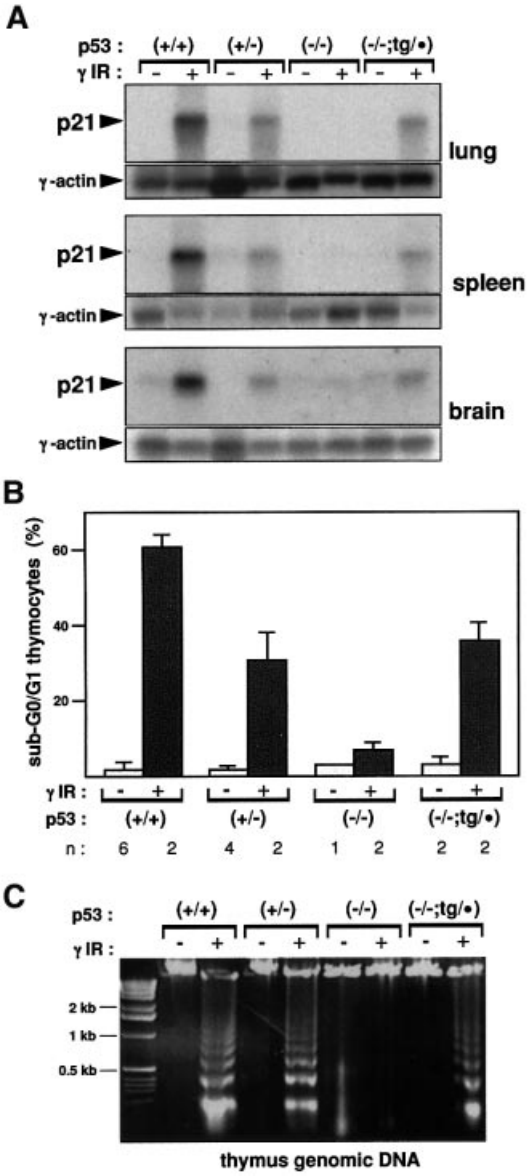

Fig. 3. Rescue of DNA damage-induced apoptosis *in vivo*. (**A**) $p53^{-/-;tg/\cdot}$ mice activate p21 in response to γ-irradiation in a manner comparable with $p53^{+/-}$ mice. Mice of the indicated genotypes were whole-body irradiated (10 Gy) or left untreated, as indicated, and, 3 h after irradiation, total RNA was extracted from the indicated organs. Northern blots were probed with murine p21 cDNA and subsequently re-probed with γ-actin. (**B**) $p53^{-/-;tg/\cdot}$ mice present a degree of radiation-induced apoptosis in the thymus similar to that of $p53^{+/-}$ mice. Mice of the indicated genotypes were whole-body irradiated (5 Gy) or left untreated, as indicated, and, 8 h after irradiation, the thymus was extracted and thymocytes were analyzed by flow cytometry to measure their DNA content and evaluate the percentage of apoptosis (<2N DNA content). Each value corresponds to the average and SD of the indicated number (*n*) of analyzed mice. (**C**) Confirmation of radiation-induced apoptosis by evaluating the appearance of a nucleosomal-derived DNA ladder. Total genomic DNA was prepared from the above-mentioned thymocyte suspensions (B) and run in agarose gels.

dosage, being able to discriminate between $p53^{+/+}$ and $p53^{+/-}$ mice (see Figure 3A). Importantly, the activation of p21 in response to γ-radiation was identical in $p53^{+/-}$ and $p53^{-/-;tg/\cdot}$ mice in all the tissues tested (Figure 3A). We also wanted to evaluate p53 functionality by measuring a more complex *in vivo* biological response, such as radiation-induced apoptosis in the thymus (Lowe *et al*., 1993). As before, this response turned out to be highly sensitive to the variations in p53 gene dosage (compare $p53^{+/+}$ and $p53^{+/-}$ mice in Figure 3B). In agreement with previous reports (Lowe *et al*., 1993), thymocyte apoptosis in response to DNA damage was entirely dependent on p53 (Figure 3B). Importantly, $p53^{-/-;tg/\cdot}$ mice had an apoptotic response that was quantitatively similar to that of $p53^{+/-}$ mice (Figure 3B). The induction of apoptosis was confirmed further by analyzing the presence of the DNA ladder characteristic of apoptotic cells (Figure 3C). In conclusion, $p53^{-/-;tg/\cdot}$ mice exhibit an apoptotic response that is essentially identical to that exhibited by $p53^{+/-}$ mice.

Summarizing this and previous sections, we have shown that the p53-tg allele is functional in all the cell types and tissues examined (including fibroblasts, thymocytes, lung, spleen and brain), responsive to a variety of stimuli signaled through the two principal routes that converge on p53 (namely DNA damage and oncogenic stress), transcriptionally active in a variety of tissues and able to exert proliferation arrest and apoptosis. Moreover, quantitative assays indicate that the degree of functionality of the p53-tg allele is comparable with, if not identical to that of the endogenous allele. Taken together, we conclude that, except for its chromosomal location (which is more prone to undergo LOH, see above), the p53-tg allele is a functional replica of the endogenous p53 gene and, therefore, $p53^{+/+;tg/\cdot}$ mice constitute a model to study the consequences of increasing p53 functionality while preserving its normal regulation.

'Super p53' mice have an enhanced response to DNA damage

Having established the functionality of the p53-tg allele, we concentrated on the analysis of $p53^{+/+;tg/\cdot}$ mice. Young and adult $p53^{+/+;tg/\cdot}$ mice were healthy and fertile, and a complete histopathological survey of 8.5-month-old $p53^{+/+;tg/\cdot}$ mice did not reveal any evidence of abnormalities or pathological processes. We next examined the response of $p53^{+/+;tg/\cdot}$ mice to DNA damage. Whole-body irradiation of these mice resulted in an enhanced activation of p21 mRNA levels compared with normal wild-type mice and in all the tissues tested (Figure 4A). Furthermore, the induction of apoptosis in the thymus was also increased in $p53^{+/+;tg/\cdot}$ mice compared with wild-type mice (Figure 4B). Note that the experimental conditions were changed in Figure 4B with respect to those in Figure 3B to allow a better quantitative discrimination. To provide the basis of confirmation with another independent mouse transgenic line, we examined the DNA damage response in the p53-tg^b line. This line, as mentioned earlier, contains two copies of BAC-p53-tg^b. Remarkably, $p53^{+/+;tg(b)/\cdot}$ mice had an even greater radiation-induced apoptotic response compared with $p53^{+/+;tg/\cdot}$ mice, as measured in both the thymus and the spleen (Figure 4C). These results are in agreement with the presence of four functional alleles of p53 in $p53^{+/+;tg(b)/\cdot}$ mice, and confirm the basic phenotype of the 'super p53' mice. Together, the above data clearly indicate that the 'super p53' mice are endowed with an enhanced p53-mediated response to DNA damage.

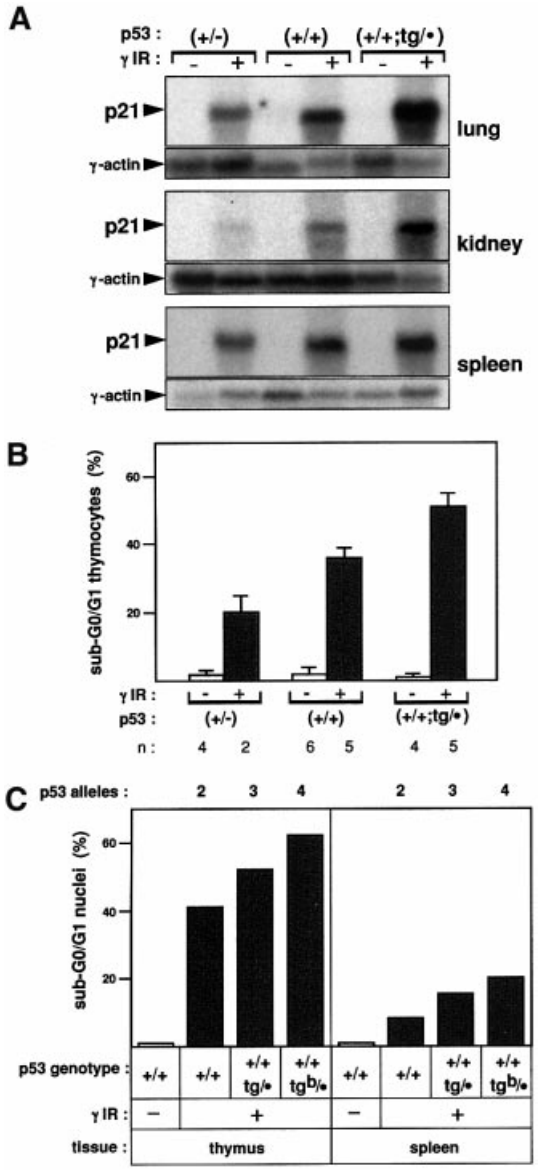

Fig. 4. 'Super p53' have a stronger response to DNA damage. (**A**) 'Super p53' ($p53^{+/+;tg/\cdot}$) mice exhibit an enhanced radiation-induced activation of p21 compared with wild-type ($p53^{+/+}$) mice. Mice of the indicated genotypes were whole-body irradiated (10 Gy) or left untreated, as indicated, and, 3 h after irradiation, total RNA was extracted from the indicated organs. Northern blots were probed with murine p21 cDNA and subsequently re-probed with γ-actin. (**B**) 'Super p53' ($p53^{+/+;tg/\cdot}$) mice exhibit an enhanced radiation-induced apoptosis in the thymus compared with wild-type ($p53^{+/+}$) mice. Mice of the indicated genotypes were whole-body irradiated (10 Gy) or left untreated, as indicated, and, 3 h after irradiation, the thymus was extracted and thymocytes were analyzed by flow cytometry to measure their DNA content and evaluate the percentage of apoptosis (<2N DNA content). Each value corresponds to the average and SD of the indicated number (*n*) of analyzed mice. (**C**) $p53^{+/+;tg-b/\cdot}$ mice exhibit an enhanced radiation-induced apoptosis in the thymus and the spleen that is consistent with four functional copies of p53. Mice of the indicated genotypes, one mouse per genotype, were treated as in (B), and both the thymus and spleen were analyzed by flow cytometry to measure the percentage of apoptosis.

'Super p53' mice are tumor resistant

The presence of an extra copy of p53 in $p53^{+/+;tg/\cdot}$ mice predicts that these mice should be tumor resistant compared with wild-type mice. We have performed chemical carcinogenesis in young healthy mice with the purpose of evaluating cancer resistance in the absence of the compounding influences that aging could have on tumorigenesis. We chose two chemical carcinogenesis protocols that induce tumors in different cell types (mesenchymal or epithelial), namely (i) induction of fibrosarcomas by acute exposure to 3-methyl-cholanthrene (3MC) (Wexler and Rosenberg, 1979); and (ii) induction of urinary bladder carcinomas by chronic exposure to *N*-butyl-*N*-(4-hydroxybutyl)nitrosamine (BBN) (Ozaki *et al*., 1998; Yamamoto *et al*., 1998). Groups of wild-type and $p53^{+/+;tg/\cdot}$ mice were subject to the above-mentioned carcinogenic regimes, and the appearance of tumors was scored. 'Super p53' mice were significantly resistant to 3MC-induced fibrosarcomas (Figure 5A and B). In fact, only four out of 12 $p53^{+/+;tg/\cdot}$ mice developed fibrosarcomas, the remaining 67% of the mice being tumor free; in contrast, 11 out 12 wild-type mice developed fibrosarcomas (Figure 5A). In the case of urinary bladder carcinomas, the protocol applied is known to produce multiple tumors per mouse bladder (~80% multifocality; see Yamamoto *et al*., 1998). In our case, about half of the wild-type mice presented multiple tumors in their bladders, whereas, in contrast, tumors in the 'super p53' mice developed with a longer latency (Figure 5C and D) and were for the most part monofocal (84%) (Figure 5E). From these data, we conclude that young 'super p53' mice have an increased resistance to the development of tumors compared with wild-type mice.

Wild-type control mice of the same genetic background as the 'super p53' mice die at an old age with an incidence of tumors of 47% (40% of these tumors were lymphomas, 30% lung adenomas, and the rest were various different types of tumors) (Figure 6B). In clear contrast, from a current population of six 'super p53' mice who died spontaneously, only one has presented a tumor (a lymphoma) (Figure 6B). The most obvious pathology observed in moribund 'super p53' mice was renal dysfunction due to glomerulonephritis, which is a common pathology in aged wild-type mice. While the population of 'super p53' that have died spontaneously is relatively limited at present (a total of six mice), the differences in tumor incidence between wild-type mice (47%) and 'super p53' mice (17%) are highly suggestive. Together, the data on chemically and spontaneously induced tumors indicate that 'super p53' mice have a significantly increased resistance to cancer.

'Super p53' mice age normally

It has been proposed that an increase in p53 functionality, while beneficial to prevent tumor development, can be detrimental to long-term viability because it may accelerate the aging process (Tyner *et al*., 2002). This proposal prompted us to evaluate the survival of the 'super p53' mice and a number of parameters associated with aging. Prior to this, and as general indicators of fitness, we evaluated the fertility and perinatal viability of the 'super p53' mice. The average litter size of crosses between 'super p53' and wild-type mice ($p53^{+/+;tg/\cdot} \times p53^{+/+}$) was 6.8 weaned mice (from a total of 22 litters), a value that was essentially identical to the average size of the litters among wild-type mice (6.5 weaned mice per litter). Also, in the above-mentioned crosses, $p53^{+/+;tg/\cdot} \times p53^{+/+}$, the

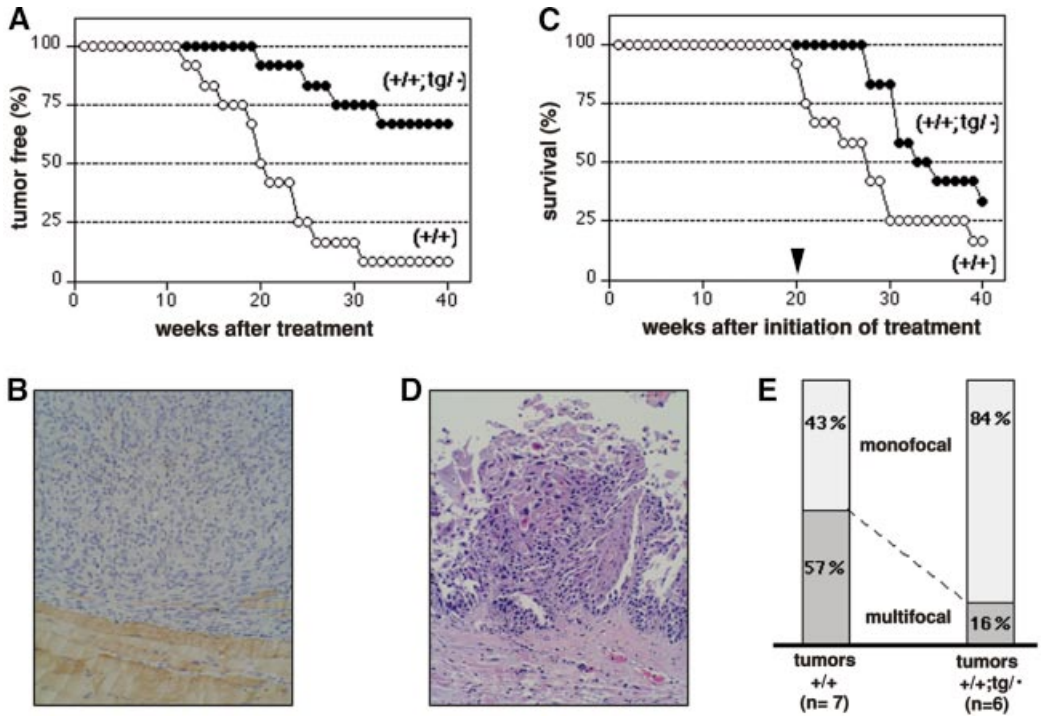

Fig. 5. 'Super p53' mice are tumor resistant. (**A**) Incidence of chemically induced fibrosarcomas in 'super p53' ($p53^{+/+;tg/\cdot}$) and wild-type ($p53^{+/+}$) mice. Fibrosarcomas were induced by a single injection of 3MC in one of the rear legs (see Materials and methods). Groups of 12 mice were used from each genotype. The time of appearance of tumors (>1.5 cm diameter) was scored. (**B**) Histopathological analysis of a fibrosarcoma. Example of a representative 3MC-induced fibrosarcoma stained with anti-desmin to reveal the infiltrated and adjacent skeletal muscle (bottom area of the field). Fibrosarcomas were highly cellular and mitotic, formed by pleomorphic spindle cells with interlacing bundles and a herring-bone pattern. Focal areas of necrosis and hemorrhages were present (data not shown). Distant metastases were not observed in any case. Original magnification 20×. (**C**) Incidence of chemically induced urinary bladder carcinomas in 'super p53' ($p53^{+/+;tg/\cdot}$) and wild-type ($p53^{+/+}$) mice. Bladder carcinomas were induced by BBN in the drinking water for 20 weeks (see Materials and methods). The arrowhead at 20 weeks indicates the termination of the treatment. Groups of 12 mice were used from each genotype. Moribund mice were sacrificed and the presence of bladder carcinomas was confirmed by histopathology (see D). (**D**) Histopathological analysis of a urinary bladder carcinoma. Example of a representative BBN-induced transitional cell carcinoma. These carcinomas were characterized by a marked proliferation of uroepithelial cells, with papillary projection into the lumen. Nests and solid sheets of depolarized cells were observed, as well as invasive epithelial cells into the stroma and the smooth muscle. Distant metastases were not observed in any case. Original magnification 20×. (**E**) Percentage of monofocal tumors in the chemically induced urinary bladder cancers.

transgene was transmitted to the viable offspring according to the expected Mendelian 1:1 ratio (the actual $p53^{+/+;tg/\cdot}$:$p53^{+/+}$ ratio from 22 litters was 72:68). Fertility and viability were identical between male and female 'super p53' mice (data not shown).

To analyze survival, we used populations of mice that had been born >2 years previously and we measured the percentage of mice that had survived for 2 years. As shown in Figure 6A, the survival fraction at 2 years was very similar among wild-type (78%) and $p53^{+/+;tg/\cdot}$ (70%), and this difference was not statistically significant (*P*-value of the *t*-test 0.62). A simple theoretical estimate based on ~50% incidence of tumors in wild-type mice and ~20% incidence in 'super p53' mice predicts a survival at 2 years of ~82% in 'super p53' mice. The fact that we do not detect this increase in survival could be due to the relatively small sample size. Preliminary survival data on a cohort of $p53^{+/+;tg/tg}$ mice (carrying four copies of p53) are also consistent with a normal lifespan (75% survival at 2 years) (Figure 6A) and, incidentally, demonstrate that the integration of the transgene has not disrupted an essential gene. Together, the lifespan of a total of 17 mice carrying extra copies of p53 (13 $p53^{+/+;tg/\cdot}$ mice and four $p53^{+/+;tg/tg}$ mice) did not show any indication of decreased survival.

It is conceivable that, despite having a normal lifespan, 'super p53' mice could age prematurely. To examine this possibility, we have analyzed a total of four biomarkers of aging, namely hair growth, lordokyphosis (hunchbacked spine), skin thickness and osteoporosis. We did not observe any decrease in the rate of hair regrowth in 'super p53' mice of 5, 12 or 19 months of age (Figure 6C). To evaluate the degree of lordokyphosis, we took whole-body X-rays (see example in Figure 6D) and used the tracings of the spine to measure its various angles. We found that the angle shown in Figure 6D was the one that correlated better with age and, in fact, we could clearly detect a narrowing of this angle with age in wild-type mice (from ~120° at 6 months to ~90° at 24 months; see Figure 6E). 'Super p53' ($p53^{+/+;tg/\cdot}$) mice, at both 6 and 24 months of age, had a similar degree of lordokyphosis when compared with wild-type mice (Figure 6E). Regarding the skin, 'super p53' and wild-type mice had a dorsal skin that was indistinguishable at both young (3 months) and old (24 months) ages (Figure 6F). The skin of aged 'super p53' mice showed the same signs of senility as the skin of aged wild-type mice, particularly a significant thinning of the subcutaneous adipose layer, a mild thinning of the dermis and partial atrophy of the hair follicles (Figure 6F). Finally, we did not observe any

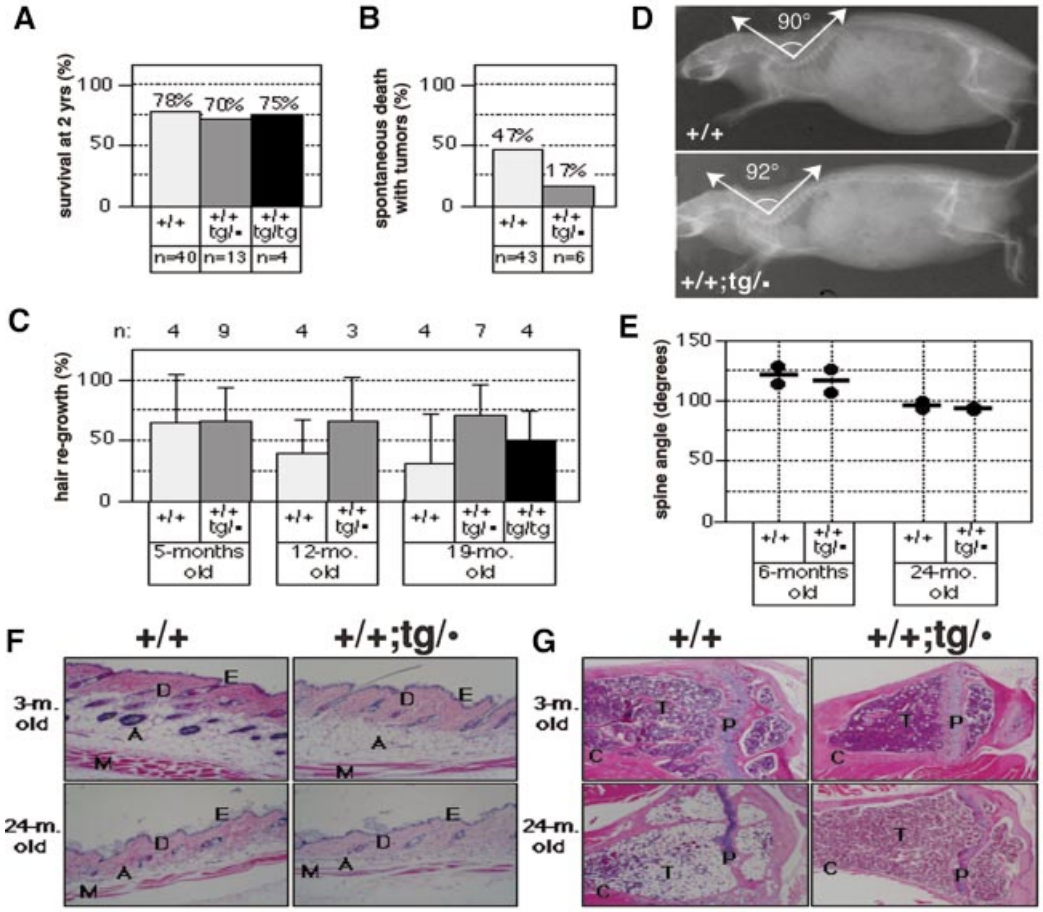

Fig. 6. 'Super p53' mice age normally. (**A**) Survival at 2 years of wild-type mice and 'super p53' mice with three ($p53^{+/+;tg/\cdot}$) or four ($p53^{+/+;tg/tg}$) p53 alleles. The genetic background of all the mice used for this measurement was mixed C57BL6:CBA, with an estimated contribution of C57BL6 of 87.5% (see Materials and methods). (**B**) Incidence of spontaneous tumors in wild-type and 'super p53' ($p53^{+/+;tg/\cdot}$) mice. Moribund mice were killed and complete histopathological surveys were performed to determine the presence of tumors. (**C**) Hair regrowth in wild-type and 'super p53' ($p53^{+/+;tg/\cdot}$ and $p53^{+/+;tg/tg}$) mice of different ages. The figure shows the average percentage of shaved area repopulated with hair after a period of 20 days since shaving. (**D**) Evaluation of lordokyphosis in aged mice. X-ray radiographs of 24-month-old male mice of the indicated genotypes. The indicated angle of the spine cord was measured to standardize the comparisons (see E). (**E**) Lordokyphosis in wild-type and 'super p53' ($p53^{+/+;tg/\cdot}$) mice of different ages. The figure shows individual measurements of the spine angle indicated in (D), in mice of different ages. A narrowing of the angle (see D) indicates an increase in lordokyphosis. (**F**) Aging of the skin in wild-type and 'super p53' ($p53^{+/+;tg/\cdot}$) mice. The figure shows representative images of hematoxylin and eosin-stained sections of the skin from the indicated mice. Two mice were analyzed per age and genotype. The epidermis (E), dermis (D), adipose layer (A) and muscular layer (M) are indicated. Mice of 2 years of age show moderate thinning of the dermis, prominent thinning of the adipose layer and atrophy of some hair follicles. Original magnification 10×. (**G**) Osteoporosis of aged wild-type and 'super p53' ($p53^{+/+;tg/\cdot}$) mice. The two top panels show representative images of hematoxylin and eosin-stained cross-sections of tibias from the indicated young mice. The two bottom panels show osteoporosis present in a fraction of wild-type (one out of three) and 'super p53' (one out of five) mice. The cortical bone (C), trabecular bone (T) and epiphyseal plate (P) are indicated. Bones with osteoporosis present thinning of the cortical bone and partial loss of the trabecular bone. Original magnification 4×.

significant differences in the bone structure of 'super p53' and wild-type mice (Figure 6G). At a young age (3 months), all the mice had a normal bone structure). Signs of osteoporosis were evident in a fraction of 2-year-old 'super p53' mice (one out of five mice analyzed) or wild-type mice (one out of three), the rest of the mice presenting a normal bone structure. Collectively, all the data obtained on viability, fertility, lifespan and aging indicate that 'super p53' mice are essentially normal and do not present accelerated aging.

Discussion

In the present work, we demonstrate the feasibility of increasing the function of the tumor suppressor p53 in the context of a mammalian organism, while, at the same time, preserving a healthy lifespan and normal aging. We have taken an approach that had not been explored before in the context of tumor suppression. This approach consists of minimally increasing the gene dosage of p53, from the normal dosage of two copies to just three copies, by introducing large genomic DNA segments containing the entire p53 gene. In this manner, it has been possible to reproduce, in an accurate manner, the behavior of the endogenous gene and, thus, to generate 'super p53' animals carrying three or four functional copies of p53. The presently described 'super p53' mice were generated with genomic transgenes that include, in addition to p53, some other genes (see Figure 1A); however, the most parsimonious explanation to account for the rescue of p53

functionality in the p53-null mice and for the DNA damage hypersensitivity and cancer resistance of the 'super p53' mice is that these phenotypes are due to p53.

We present a variety of evidence demonstrating that 'super p53' mice have an enhanced response to DNA damage. Examination of quantitative assays suggests that there is a linear correlation between the gene dosage of p53 and the enhancement of the DNA damage response in two independent transgenic mouse lines (see Figure 4C). This outcome was not necessarily anticipated because, in principle, the negative feedback loop formed by p53 and MDM2 could influence significantly the quantitative relationship between p53 gene dosage and p53-dependent responses (Lev Bar-Or *et al*., 2000). Our observations suggest that p53-dependent responses to DNA damage are closely proportional to the number of p53 functional alleles.

The tumor resistance phenotype of the 'super p53' mice is probably the result of the additive contribution of two components. On one hand, upon cellular damage, p53-dependent responses are exacerbated, providing a more robust control of the damaged cells and, therefore, impairing the emergence of tumoral cells. On the other hand, the simple fact that there are more p53 gene copies implies that the probability of p53 inactivation by stochastic mutations is significantly decreased. We anticipate that the contribution of each of the above factors will vary among different tumor types, thus yielding a final increase in cancer protection quantitatively different for each tissue type. In any case, it should be noted that 'super p53' mice may eventually develop tumors although with longer latency and lower penetrance, and, in the immediate future, it will be of interest to characterize the genetic alterations present in these tumors in relation to p53.

Recently, a role for p53 in organismal aging has been proposed based on the analysis of mice carrying mutant versions of p53 (Tyner *et al*., 2002). Significantly, these mutant alleles probably provide levels of constitutively activated p53 (Tyner *et al*., 2002). It is conceivable that constitutive or highly frequent activation of p53, such as under chronic exposure to stress, could result in accelerated aging. In contrast, 'super p53' mice have a normal aging process despite having clearly increased p53 functionality. A critical characteristic of the 'super p53' mice is the fact that the basal levels of p53 activity are not affected (see Figures 2B and 4). The exercise of further increasing the gene dosage of p53 will certainly be informative and may eventually reveal a threshold at which deleterious effects will be noticeable, probably in the form of defective tissue regeneration, growth atrophies and premature aging. In summary, we propose that increases in normally regulated p53, as in the 'super p53' mice, confer cancer protection without affecting aging, whereas, in contrast, constitutive levels of active p53 provide cancer protection but promote aging.

Our present work demonstrates that cancer resistance is a flexible trait that can be enhanced by a simple genetic modification and in the absence of obvious secondary effects. The possibility of enhancing cancer resistance is a proof of principle for similar, or better tailored, modifications that could be introduced *ex vivo* into stem cells with the purpose of improving their cancer resistance prior to therapeutic transplantation. Prompted by the recent generation of transgenic primates (Chan *et al*., 2001), we cannot avoid making reference to current discussions about the many implications that human germline modification could have (Frankel and Chapman, 2001; Knight, 2001; Resnik and Langer, 2001). While these discussions generally consider abstract or highly controversial genetic modifications, our transgenic mice provide a prime example of a gene modification conferring a phenotype generally regarded as beneficial, i.e. cancer protection. In any case, we anticipate that further transgenesis experimentation along the lines of this work will significantly advance our understanding of and ability to manipulate cancer resistance.

Materials and methods

BAC isolation and characterization

Large genomic DNA segments containing the murine p53 gene were identified by screening a commercial BAC murine genomic library ('Down-to-the-Well', Genome Systems) derived from embryonic stem cells (129Sv genetic background) and cloned into BAC vector pBeloBAC11. The library was screened by PCR, following the instructions of the vendor, and using a PCR that amplifies intron 6 with primers W5′ and W3′, which hybridize to exons 6 and 7, respectively, as previously reported (Jacks *et al*., 1994). Two BAC-p53s were obtained, and their terminal sequences (~500 bp) were determined by sequencing with primers complementary to the insert-flanking regions of the vector, namely SP6-BAC (5′-GCTATGACCATGATTACGCCAAG-3′) and T7-BAC (5′-TAATACGACTCACTATAGGG-3′). These terminal sequences were compared with the ENSEMBL Mouse Genome Database and, in this manner, it was possible to determine unequivocally the position of the genomic inserts. The BAC vector pBeloBAC11 contains *Not*I sites flanking the genomic insert. This convenient feature was used to determine, by pulsed-field gel electrophoresis, that the insert size was compatible with that predicted from the ESEMBL Mouse Genome Database, and that both BAC-p53s inserts were devoid of internal *Not*I sites.

Transgenesis

For transgenesis, the two BAC-p53s were digested with *Not*I, thus liberating the genomic insert together with short vector flanking segments containing the SP6 and T7 hybridization sites. BACs were purified from bacteria using a standard plasmid preparation protocol, and the final stocks were quantified by spectroscopy. The BAC DNA preparations were digested with *Not*I and, after heat inactivation, the mixtures were diluted in microinjection buffer (10 mM Tris–HCl pH 7.5, 0.1 M NaCl, 0.1 mM EDTA, 30 μM spermine, 70 μM spermidine), at a final concentration of 1 ng/μl. After filtration (0.22 μm pore) and centrifugation (15 000 *g* for 10 min at room temperature), the mixture was used for microinjection. Pronuclei of fertilized oocytes, derived from intercrosses between (C57BL/6 × CBA)F_1 mice, were injected with ~2 pl of the DNA solution. Microinjected eggs were cultured in M16 medium drops, at 37°C and 5% CO_2, for 20–24 h. Subsequently, embryos at the two-cell stage were transferred into the oviducts of recipient pseudopregnant CD1 females. The resulting offspring were analyzed for the presence of the transgene using PCRs that detected the junction between the SP6 and T7 vector flanking elements and the genomic insert. For BAC-p53-tg, we used: for the SP6 terminus, primers SP6-BAC (see above) and SP6-tg (5′-CTAAGTCCCTCTGCATGTGG-3′); and for the T7 terminus, T7-BAC (see above) and T7-tg (5′-GAGTCAGGGGTGG-GAACTTGG-3′). For BAC-p53-tg^b, we used: for the SP6 terminus, primers SP6-BAC (see above) and SP6-tg-b (5′-TTGAAACTGC-TAAATGCTGGA-3′); and for the T7 terminus, T7-BAC (see above) and T7-tg-b (5′-CCAAGTTGCTACGTTCCTGAA-3′). Genotyping using Southern blotting is described in detail in the Supplementary data available at *The EMBO Journal* Online.

Mouse breeding and maintenance

Mice were housed at the Spanish National Center of Biotechnology, Madrid, in a pathogen-free barrier area. Mice were killed humanely in accordance with the Guidelines for Humane Endpoints for Animals Used in Biomedical Research. Mice derived from microinjected oocytes were analyzed by PCR (see above), using tail-tip DNA to detect the presence of

the transgene. For transgene p53-tg, one carrier was identified by PCR out of a total of 17 microinjected mice, and this carrier transmitted the transgene to its progeny. For transgene p53-tg^{b}, four carriers were identified by PCR out of a total of 73 microinjected mice, and only one carrier transmitted the transgene to its progeny.

All the 'super p53' mice used in this work were derived from C57BL6:CBA (50%:50%) mice subsequently backcrossed two, three or four times with C57BL6, thus of a mixed genetic background C57BL6:CBA, with an estimated contribution of 87.5, 93.75 or 96.8% of C57BL6, respectively. To evaluate the functionality of the transgenes, carrier mice were crossed with p53-null mice (Jacks *et al*., 1994). These p53-null mice were of either pure C57BL6 background or mixed C57BL6:129Sv (50%:50%) genetic background. Thus the resulting mice had complex genetic backgrounds, but in all cases the predominant genetic background was C57BL6 (>50%). All the experiments were performed by comparing mice of the same genetic background carrying or not carrying the p53 transgenes. Furthermore, in the cases of radiation sensitivity, we confirmed experimentally that the responses were quantitatively indistinguishable among mice that had a C57BL6 component >50% (the rest of the genetic background being 129Sv or CBA) and up to 100% C57BL6. In the case of chemical carcinogenesis, the responses were identical (same latency for 3MC-induced tumors, and same multifocality for BBN tumors) between control mice that were 93.75% C57BL6 or 100% C57BL6.

Assays with MEFs

Isolation, culture and assays with MEFs were performed as described previously (Brugarolas *et al*., 1995; Pantoja and Serrano, 1999; see Supplementary data).

Chemical carcinogenesis

For the induction of fibrosarcomas, cohorts of p53$^{+/+;tg/}$ mice (n = 12) and p53$^{+/+}$ mice (n = 12), of both sexes, and of 3–5 months of age, received a single intramuscular injection, in one of the rear legs, of a 40 µl solution containing 3MC (Aldrich), at a concentration of 25 µg/µl, and dissolved in sesame oil (Sigma), as described previously (Wexler and Rosenberg, 1979). Mice were observed on a daily basis until tumors of >1.5 cm in diameter developed in the injected leg, at which point the animals were killed humanely and the tumors were extracted for further analysis. For the induction of urinary bladder carcinomas, mice of 3–5-months of age were exposed to BBN (TCI, Japan) permanently present in the drinking water at a concentration of 0.025%, during 20 weeks, as described previously (Ozaki *et al*., 1998; Yamamoto *et al*., 1998). Mice were observed on a daily basis and they were killed humanely when they manifested signs of morbidity. Upon necropsy, tumors in the urinary bladder were evident and the entire urinary system, including the kidneys, was extracted for further analysis.

Radiation of mice, histopathology and aging biomarkers

These procedures were performed following standard protocols as described previously (Macleod *et al*., 1995; Tyner *et al*., 2002; see Supplementary data).

Supplementary data

Supplementary data are available at *The EMBO Journal* Online.

Acknowledgements

We thank Dr Lluis Montoliu (CNB) for his input and criticisms, and Dr Pilar Llorens-Pena (Veterinary School of Complutense University) for her advice. I.G.-C. and M.G.-C. are recipients of pre-doctoral fellowships from the Spanish Ministries of Education and Culture, and Science and Technology, respectively. This work was funded by grants PM98-0124 (National Plan for Science and Technology, Spain) and QLRT-2000-02084 (LIFE Program, European Union), to M.S. The Department of Immunology and Oncology, at the CNB, was founded and is supported by a consortium between the CSIC and Pharmacia Corporation.

References

Allemand,I., Anglo,A., Jeantet,A.Y., Cerutti,I. and May,E. (1999) Testicular wild-type p53 expression in transgenic mice induces spermiogenesis alterations ranging from differentiation defects to apoptosis. *Oncogene*, **18**, 6521–6530.

Brugarolas,J., Chandrasekaran,C., Gordon,J.I., Beach,D., Jacks,T. and Hannon,G.J. (1995) Radiation-induced cell cycle arrest compromised by p21 deficiency. *Nature*, **377**, 552–557.

Chan,A.W., Chong,K.Y., Martinovich,C., Simerly,C. and Schatten,G. (2001) Transgenic monkeys produced by retroviral gene transfer into mature oocytes. *Science*, **291**, 309–312.

Deng,C., Zhang,P., Harper,J.W., Elledge,S.J. and Leder,P. (1995) Mice lacking p21CIP1/WAF1 undergo normal development, but are defective in G_1 checkpoint control. *Cell*, **82**, 675–684.

Frankel,M.S. and Chapman,A.R. (2001) Genetic technologies. Facing inheritable genetic modifications. *Science*, **292**, 1303.

Giraldo,P. and Montoliu,L. (2001) Size matters: use of YACs, BACs and PACs in transgenic animals. *Transgenic Res.*, **10**, 83–103.

Godley,L.A., Kopp,J.B., Eckhaus,M., Paglino,J.J., Owens,J. and Varmus,H.E. (1996) Wild-type p53 transgenic mice exhibit altered differentiation of the ureteric bud and possess small kidneys. *Genes Dev.*, **10**, 836–850.

Hanahan,D. and Weinberg,R.A. (2000) The hallmarks of cancer. *Cell*, **100**, 57–70.

Harvey,M. *et al*. (1993a) *In vitro* growth characteristics of embryo fibroblasts isolated from p53-deficient mice. *Oncogene*, **8**, 2457–2467.

Harvey,M., McArthur,M.J., Montgomery,C.A.,Jr, Butel,J.S., Bradley,A. and Donehower,L.A. (1993b) Spontaneous and carcinogen-induced tumorigenesis in p53-deficient mice. *Nature Genet.*, **5**, 225–229.

Jacks,T., Remington,L., Williams,B.O., Schmitt,E.M., Halachmi,S., Bronson,R.T. and Weinberg,R.A. (1994) Tumor spectrum analysis in *p53*-mutant mice. *Curr. Biol.*, **4**, 1–7.

Knight,J. (2001) Biology's last taboo. *Nature*, **413**, 12–15.

Lev Bar-Or,R., Maya,R., Segel,L.A., Alon,U., Levine,A.J. and Oren,M. (2000) Generation of oscillations by the p53–Mdm2 feedback loop: a theoretical and experimental study. *Proc. Natl Acad. Sci. USA*, **97**, 11250–11255.

Lowe,S.W., Schmitt,E.M., Smith,S.W., Osborne,B.A. and Jacks,T. (1993) p53 is required for radiation-induced apoptosis in mouse thymocytes. *Nature*, **362**, 847–849.

Macleod,K.F., Sherry,N., Hannon,G., Beach,D., Tokino,T., Kinzler,K., Vogelstein,B. and Jacks,T. (1995) p53-dependent and independent expression of p21 during cell growth, differentiation and DNA damage. *Genes Dev.*, **9**, 935–944.

Nakamura,T., Pichel,J.G., Williams-Simons,L. and Westphal,H. (1995) An apoptotic defect in lens differentiation caused by human p53 is rescued by a mutant allele. *Proc. Natl Acad. Sci. USA*, **92**, 6142–6146.

Ozaki,K. *et al*. (1998) High susceptibility of *p53*$^{+/-}$ knockout mice in *N*-butyl-*N*-(4-hydroxybutyl)nitrosamine urinary bladder carcinogenesis and lack of frequent mutation in residual allele. *Cancer Res.*, **58**, 3806–3811.

Palmero,I., Pantoja,C. and Serrano,M. (1998) p19^{ARF} links the tumour suppressor p53 to Ras. *Nature*, **395**, 125–126.

Pantoja,C. and Serrano,M. (1999) Murine fibroblasts lacking p21 undergo senescence and are resistant to transformation by oncogenic Ras. *Oncogene*, **18**, 4974–4982.

Prives,C. and Hall,P.A. (1999) The p53 pathway. *J. Pathol.*, **187**, 112–126.

Resnik,D.B. and Langer,P.J. (2001) Human germline gene therapy reconsidered. *Hum. Gene Ther.*, **12**, 1449–1458.

Serrano,M. and Blasco,M.A. (2001) Putting the stress on senescence. *Curr. Opin. Cell Biol.*, **13**, 748–753.

Serrano,M., Lin,A.W., McCurrach,M.E., Beach,D. and Lowe,S.W. (1997) Oncogenic ras provokes premature cell senescence associated with accumulation of p53 and p16^{INK4a}. *Cell*, **88**, 593–602.

Shao,C., Deng,L., Henegariu,O., Liang,L., Raikwar,N., Sahota,A., Stambrook,P.J. and Tischfield,J.A. (1999) Mitotic recombination produces the majority of recessive fibroblast variants in heterozygous mice. *Proc. Natl Acad. Sci. USA*, **96**, 9230–9235.

Sharpless,N.E. and DePinho,R.A. (1999) The *INK4A/ARF* locus and its two gene products. *Curr. Opin. Genet. Dev.*, **9**, 22–30.

Sherr,C.J. (1998) Tumor surveillance via the ARF–p53 pathway. *Genes Dev.*, **12**, 2984–2991.

Sherr,C.J. and DePinho,R.A. (2000) Cellular senescence: mitotic clock or culture shock? *Cell*, **102**, 407–410.

Tsukada,T. *et al*. (1993) Enhanced proliferative potential in culture of cells from p53-deficient mice. *Oncogene*, **8**, 3313–3322.

Tyner,S.D. *et al*. (2002) p53 mutant mice that display early ageing-associated phenotypes. *Nature*, **415**, 45–53.

Vogelstein,B., Lane,D. and Levine,A.J. (2000) Surfing the p53 network. *Nature*, **408**, 307–310.

Wang,Y.A., Elson,A. and Leder,P. (1997) Loss of p21 increases sensitivity to ionizing radiation and delays the onset of lymphoma in atm-deficient mice. *Proc. Natl Acad. Sci. USA*, **94**, 14590–14595.

Wexler,H. and Rosenberg,S.A. (1979) Pulmonary metastases from autochthonous 3-methylcholanthrene-induced murine tumors. *J. Natl Cancer Inst.*, **63**, 1393–1395.

Woods,D.B. and Vousden,K.H. (2001) Regulation of p53 function. *Exp. Cell Res.*, **264**, 56–66.

Xu,Y., Yang,E.M., Brugarolas,J., Jacks,T. and Baltimore D. (1998) Involvement of p53 and p21 in cellular defects and tumorigenesis in $Atm^{-/-}$ mice. *Mol. Cell. Biol.*, **18**, 4385–4390.

Yamamoto,S., Tatematsu,M., Yamamoto,M., Fukami,H. and Fukushima,S. (1998) Clonal analysis of urothelial carcinomas in C3H/HeN↔BALB/c chimeric mice treated with *N*-butyl-*N*-(4-hydroxybutyl)nitrosamine. *Carcinogenesis*, **19**, 855–860.

Received July 31, 2002; revised and accepted September 19, 2002